Long-Range Order in Alloys

In many alloys, the positions of the different species of atoms are not random; that is, the probability that a pair of sites is occupied by specific atoms is not equal to the random probability obtained by multiplying their respective atomic fractions. If such "ordering" only occurs over regions approximately several times the interatomic distances, the order is usually termed short range or local (see *Local Order in Crystalline Alloys*). If the ordering persists over distances which are large compared to the interatomic distance, the ordering is denoted long-range order (LRO). In this article, the concepts of domains and variants are introduced on the basis of symmetry change and various ordered structures are presented, together with a discussion of their stability. Finally, a brief discussion of how the symmetry of ordered phases affects deformation is presented. This article replaces the article of the same title in the Main Encyclopedia.

1. Symmetry

A crystal consists of a large number of atoms arranged periodically in space. Its symmetry may be divided into two types: symmetry about a point and translational symmetry. When the atoms of a binary alloy "order" (that is, arrange themselves on specific sites), some symmetry is lost.

For some types of ordering, the point-group symmetry of the disordered phase does not change; only the translational symmetry changes. Two examples of this type of ordering shown in Fig. 1 are the

$$\mathrm{A1}(Fm\bar{3}m) \rightarrow \mathrm{L1_2}(Pm\bar{3}m) \qquad (1)$$

and the

$$\mathrm{A2}(Im\bar{3}m) \rightarrow \mathrm{B2}(Pm\bar{3}m) \qquad (2)$$

ordering reactions. In both cases, the point-group

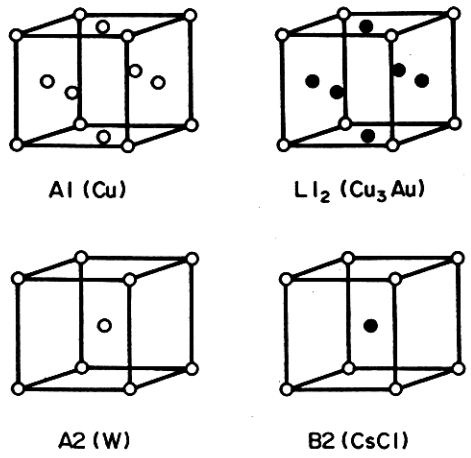

Figure 1
Disordered and ordered crystal structures

symmetry, and hence the crystal class, stays the same. Also, the same size unit cell can be used to represent both the disordered and ordered structures. However, the number of equivalent positions within the unit cell decreases; that is, the translational symmetry of the structure decreases. This decrease in translational symmetry (for cases where the unit-cell size stays the same) can be quantified by noting the change in the number of Bravais lattice points of the crystal resulting from ordering. For the $L1_2$ structure, the translational symmetry is decreased by a factor of four, while for the B2 structure, translational symmetry is decreased by a factor of two.

This loss of translational symmetry manifests itself in an increase in the density of reciprocal lattice nodes with nonzero scattered intensity. For these two ordering reactions, the increase in the number of diffraction "spots" per unit volume of reciprocal space is four and two, respectively (see Fig. 2; note that these numbers are the same as those for the decrease in translational symmetry). These new reflections are termed "superlattice" reflections. Reflections from the disordered crystal (higher symmetry) are called fundamental reflections. The superlattice reflections are usually of lower intensity than the fundamental reflections.

The decrease in translational symmetry also manifests itself in real space by the formation of ordered domains. Consider the transition (2). The A atoms may be situated either at the corners of the B2 unit cell (and hence on the Bravais lattice points) or at the center of the unit cell ($\frac{1}{2}[111]$ from the Bravais lattice points). These represent two possible domains of the ordered phase. The domains are related to each other by the translational symmetry element that was lost; that is, $\frac{1}{2}\langle 111\rangle$. Similarly, it can be shown that for the case of $A1 \rightarrow L1_2$ ordering, four domains exist, related to one another by $\frac{1}{2}\langle 110\rangle$. These domains can have a strong influence on properties of the ordered phase (see *Ordered Alloys: Mechanical Properties*).

In a different type of ordering, the rearrangement of atoms produces a crystal with a new point-group symmetry. A new crystal class may be formed. A simple example of this is the $A1(Fm\bar{3}m) \rightarrow L1_0(P4/mmm)$ case shown in Fig. 3. Here, the point-group symmetry has decreased by a factor of three, from order 48 for the point group $m\bar{3}m$ to 16 for the point group $4/mmm$. Also, the translational symmetry has decreased by a factor of two. The decrease in translational symmetry produces two domains for each of the variants of the ordered structure. The decrease in point-group symmetry produces three possible crystallographic variants shown in Fig. 4. This is demonstrated by noting that the tetragonal axis may be along any of the three 4-fold axes of the disordered cubic crystal. For each of these crystallographic variants there exist two domains.

Crystal structures, such as those just noted, that are formed from other structures by reducing the number of symmetry elements while maintaining the approximate relative positions (not necessarily identity) of atoms, are called derivative crystal structures. The higher symmetry (disordered) structure is usually the one that is present at high temperatures. Phase transformations involving derivative crystal structures have the important property that complete lattice registry (coherency) can be maintained across the interphase interfaces of the disordered and ordered phases. This coherency is often accompanied by a strain, which makes these two-phase alloys capable of "precipitation hardening." In addition, their coherent interface implies a low interphase surface energy, further implying relative stability of the phase with respect to coarsening.

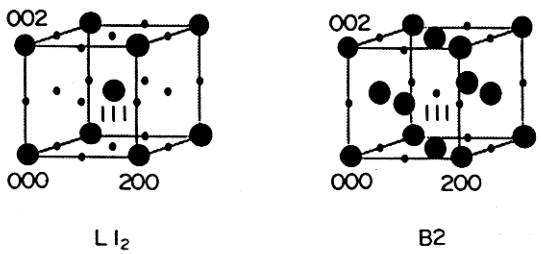

Figure 2
Reciprocal space intensity distribution for the $L1_2$ and B2 real space structures

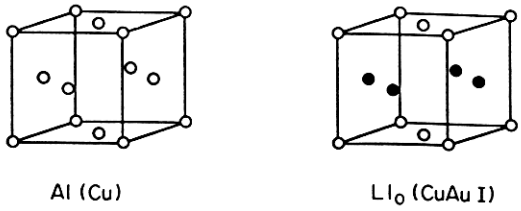

Figure 3
The $L1_0$ (CuAuI) structure and its parent structure (A1)

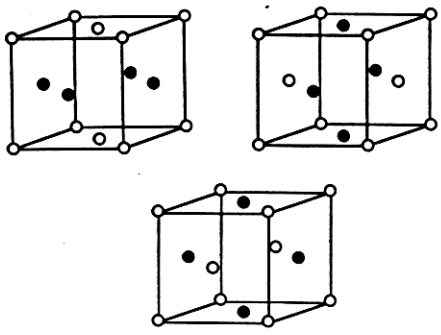

Figure 4
The three possible crystallographic variants for the $L1_0$ structure

2. Statistical Treatment of Equilibrium Phases

The most likely arrangement of atoms on their crystal sites can be calculated, in principle, by the use of statistical thermodynamics. The equilibrium state is the most likely state, and this can be determined by finding an expression for the partition function Z of the system, defined as

$$Z = \sum_i \omega_i \exp\left(\frac{E_i}{kT}\right) \tag{3}$$

where ω_i is the number of configurations with the same energy E_i, and k and T are Boltzmann's constant and temperature, respectively. The sum is over all energy levels. This value is related to the free energy of the system by the equation

$$F = -kT \ln Z \tag{4}$$

Naturally, it is very difficult to find the value of Z for systems which contain a large number of atoms. Various approximations are usually made, such as the neglect of vibrational energy and the use of pairwise interactions exclusively. To date, only the one- and two-dimensional cases have been solved exactly. High- and low-temperature expansions have been utilized to find analytical expressions for Z and Monte Carlo techniques have been used to solve numerically for Z. The cluster variation method (CVM) introduced by Kikuchi (1951) can be used to calculate phase equilibria. By this method, clusters of atoms of different composition are placed on the lattice and the most probable arrangement is determined. This technique is essentially an extension of the method of Bethe in his extension of the zeroth order approximation to the partition function.

3. Ground-State Diagrams

Richards and Cahn (1971) have derived ground state ($T = 0$ K) diagrams for body-centered cubic (bcc) and face-centered cubic (fcc) derivative structures, taking into account first- and second-neighbor interactions. We will only consider bcc derivative structures in detail. All of the bcc derivative structures to be discussed can be visualized with the aid of Fig. 5. Here, the bcc structure is extended and can be seen to be composed of four interpenetrating fcc sublattices, denoted α, β, γ and δ. Table 1 lists possible compositions of these sublattices, along with the structures which result when the compositions are as denoted. These are the possible ground-state structures of bcc derivative structures. The bcc ground-state diagram is shown in Fig. 6. This diagram shows that an alloy of 50%A and 50%B will have the CsCl structure if $V_2/V_1 < 2/3$, where V_i is the ith neighbor interaction action energy, and V_1 is assumed negative, that is, favoring ordering. The CsCl structure has all opposite first neighbors ($\frac{1}{2}\langle 111\rangle$) and all second neighbors that are of the same type ($\langle 100\rangle$)

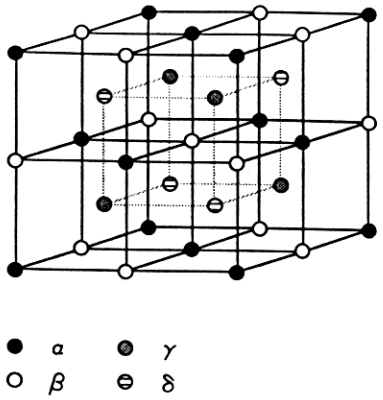

Figure 5
Extended bcc structure, showing that it is composed of four interpenetrating fcc lattices

Table 1
Possible combinations of interpenetrating fcc sublattices along with their resulting structures

Sublattice					
α	β	γ	δ	Structure (prototype)	Space group
A	A	A	A	A2(W)	$Im\bar{3}m$
A	A	B	B	B2(CsCl)	$Pm\bar{3}m$
B	A	A	A	$DO_3(BiF_3)$	$Fm\bar{3}m$
A	B	A	B	B32(NaTl)	$Fd\bar{3}m$

(see Fig. 1). If $V_2/V_1 > 2/3$, the second-neighbor interaction becomes dominant; a structure with opposite second neighbors will be favored. The B32(NaTl) structure fulfills this requirement. It has four opposite near neighbors and four near neighbors of the same atom. In contrast to the B2(CsCl) structure, however, it has six second neighbors that are opposite, that is, all second neighbors are opposite.

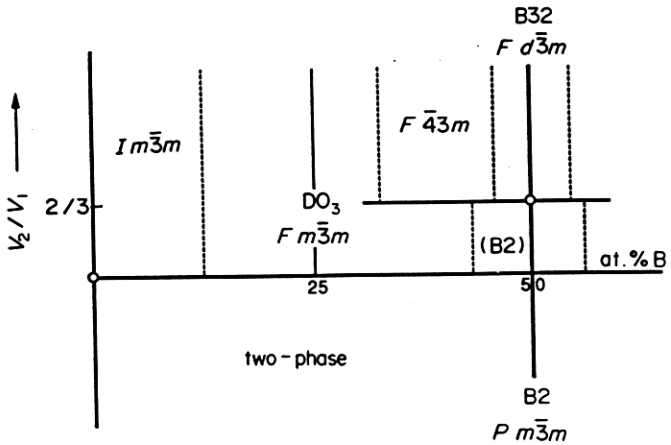

Figure 6
Ground-state phase diagram for bcc derivative structures

Thus, the NaTl structure is stable relative to the CsCl structure for $V_2/V_1 > 2/3$.

For bcc-based alloys with 25%B, the equilibrium state for $V_2/V_1 < 0$ is two-phase: bcc and CsCl. If all the B atoms cluster into one region and form the ordered CsCl phase, all second neighbors of the B atoms will be A (as favored since $V_2 > 0$). A single phase with B atoms randomly distributed could not guarantee all opposite first neighbors for B or all similar second neighbors for B. However, if $V_2/V_1 > 0$ (favoring opposite second neighbors), the ground state for the 25%B alloy is DO_3, since this structure has all opposite second neighbors for the B atoms.

A similar diagram has been derived for fcc derivative structures. Here, $L1_2(Cu_3Au)$ is the equilibrium phase for $V_2/V_1 < 0$ (25%B) and $Li_0(CuAuI)$ is the ground state for a 50%B alloy with a similar ratio of second- to first-neighbor interaction energies. For $V_2/V_1 > 0.5$, structures in which second neighbors are opposite become the ground state ones. Thus the DO_{22} structure (Al_3Ti) is ground state for 25%B alloys and $L1_1$(CuPt) for 50%B alloys. These ground states have also been derived by Monte Carlo techniques.

4. *Diamond Structure Derivatives*

With the increase in studies of semiconductor materials, a new set of superlattice structures has become important. These are the structures which are crystallographic derivatives of the diamond cubic structure $Fd\bar{3}m$ (see Fig. 7a). The most widely known derivative structure of diamond cubic is the zinc blende structure ($F\bar{4}3m$), also termed sphalerite (see Fig. 7b). This is the structure of GaAs, InP and most other III–V compounds. For zinc blende, the atoms at the face-centered cubic Bravais lattice points are of one type, and the atoms away from the Bravais lattice points are of another type. This structure is not centrosymmetric, so that materials with this structure behave differently in some aspects from those with the diamond cubic structure.

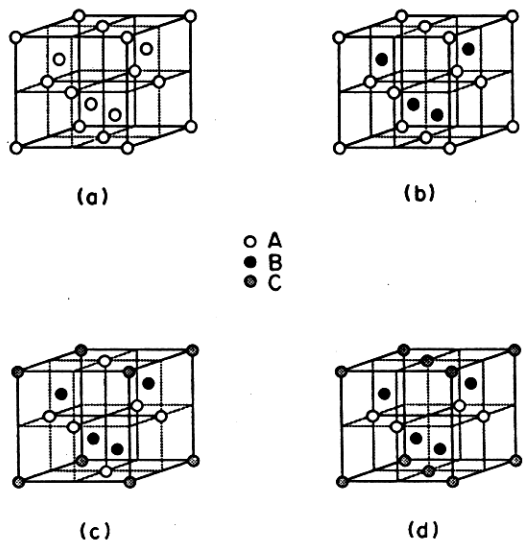

Figure 7
(a) Diamond cubic structure (A4), (b) zinc blende (B4), (c) $P\bar{4}3m$, (d) $P\bar{4}2m$

More superstructures based on the diamond cubic structure are possible. For example, if a ternary addition C replaces all of the A atoms on the corner sites of the fcc Bravais lattice, a structure related to that of $Cu_3Au(L1_2)$ is formed (see Fig. 7c). This structure has the space group $P\bar{4}3m$. For complete substitution, the stoichiometry would be $A_{0.75}C_{0.25}B$. Another structure which can form is shown in Fig. 7d. Here the A atoms at sites (000) and $(\frac{1}{2}\frac{1}{2}0)$ are replaced by C atoms, yielding a structure with tetragonal symmetry ($P\bar{4}2m$). This structure has the ideal stoichiometry $A_{0.5}C_{0.5}B$. More complex ordering is, of course, possible. Structures based on the fcc derivative structures $Al_3Ti(DO_{22})$ and $CuPt(L1_1)$ have been reported. Also, quaternary additions could substitute on the B sublattice, so that both sublattices may be "ordered."

5. *Order–Disorder*

The order–disorder (O–D) transition has a long history of experimental and theoretical interest. The first structural studies on ordered phases were done in the early 1920s. (Remember that x rays were discovered in 1896, and it was only in 1912 that their wavelike character was demonstrated.) In the 1930s, Ehrenfest proposed a thermodynamic classification of phase transitions into first-, second- and third-order transitions and so on. According to this scheme, the "order" of a transition is the order of the derivative of the free energy with respect to a state variable, which first becomes discontinuous at the transition temperature. It is now more common to speak of only first-order and higher-order transitions. It is an established fact that the atomic ordering transition for some alloys is "first order," while for others it is "higher order." A basic distinction of these two types of transitions is the way that the ordering reaction proceeds at the transition temperature. If, at the transition temperature, the disordered phase and ordered phase can be distinguished and can be held in equilibrium, the reaction is classified as first order. If it is impossible to distinguish between the ordered and disordered phase at the transition temperature, the transition is of "higher order." A measure of the order in an alloy is the long-range order parameter η, defined as $\eta = |f_{r\alpha} - f_{w\beta}|$ where $f_{r\alpha}$ is the fraction of α sites that are rightly occupied, and $f_{w\beta}$ is the fraction of β sites that are wrongly occupied. For stoichiometric alloys this parameter ranges between zero (complete disorder) and unity (complete order). Experimentally, two

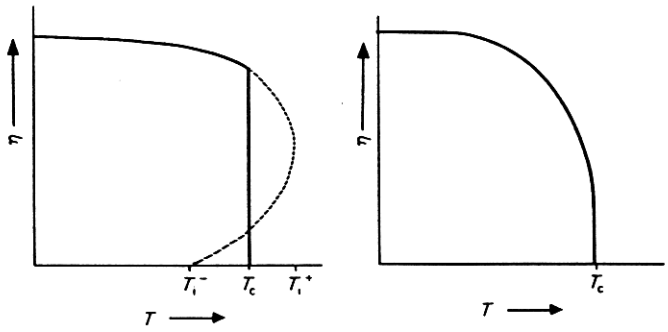

Figure 8
Long-range order (η) against temperature (T) curves for (a) first-order transition, (b) higher-order transition

types of η against T curves are observed. These are shown schematically in Fig. 8. Note that η approaches zero continuously for higher-order transitions, while it has a discontinuity for first-order transitions.

Following Landau and Lifshitz (1978), the free energy of a system may be expressed in terms of the expansion in η about the critical temperature:

$$F = F_0 + \left(\frac{\partial F}{\partial \eta}\right)\eta + \left(\frac{\partial^2 F}{\partial \eta^2}\right)\eta^2 + \cdots \qquad (5)$$

where F_0 is the free energy of the disordered phase ($\eta = 0$) and F is the free energy of the ordered phase.

If the system is stable at T_c, $\partial F/\partial \eta = 0$, so to first order:

$$F = F_0 + \left(\frac{\partial^2 F}{\partial \eta^2}\right)\eta^2 \qquad (6)$$

For a continuous transition to occur at the critical temperature, $F = F_0$, or $(\partial^2 F/\partial \eta^2) \equiv 0$. This is a general criterion: a system changes phase continuously if the second derivative of its free energy with respect to the appropriate order parameter is zero.

6. *Stability of Ordered Phases*

A basic difference between first-order and higher-order transitions is with regard to the instability of the various phases that are present. In higher-order transitions, the disordered phase (on cooling) becomes unstable with respect to the formation of the ordered phase at the same temperature at which the ordered phase (on heating) becomes unstable with respect to the formation of the disordered phase. This temperature is called the transition temperature, and on phase diagrams it is usually "hatched" to indicate that it is of higher order. Differential scanning calorimetry (DSC) of an alloy undergoing such a transition should look similar for both heating and cooling.

On the other hand, for first-order transitions, the instability temperatures of the ordered phase (T_i^+) and of the disordered phase (T_i^-) are different. If one considers the η against T curve for a first-order transition, shown in Fig. 8, one can see that the ordered phase can be heated above T_c to the temperature T_i^+ before becoming unstable with respect to disordering. On cooling, the disordered phase can be brought to T_i^- before becoming unstable with respect to ordering. Thus for the case of a stoichiometric alloy, the following relation holds:

$$T_i^- < T_c < T_i^+ \qquad (7)$$

where T_c is the transition temperature of the first-order transition.

A schematic phase diagram of a first-order O–D transformation is shown in Fig. 9, in which x_B denotes the mole fraction. A disordered alloy quenched from high temperature into the two-phase field is metastable with respect to the formation of the ordered phase, if held at $T > T_i^-$. This means that the ordered phase must nucleate if it is to form. If the disordered phase is quenched below T_i^- it is unstable with respect to homogeneous ordering; the entire phase orders without a thermodynamic barrier. After homogeneous ordering, the single ordered phase will decompose into two phases, one of which becomes disordered when its composition passes through the T_i^+ curve. On heating a two-phase mixture of the equilibrium disordered and ordered phases, the ordered phase should dissolve into the matrix. This process should be complete when the temperature reaches the phase boundary. If, however, the alloy is heated too rapidly, the ordered phase may not have sufficient time to dissolve; rather, it may disorder when its temperature reaches T_i^+ for the composition of the ordered phase. Such nonequilibrium transitions must be kept in mind when interpreting DSC/DTA (differential thermal analysis) scans.

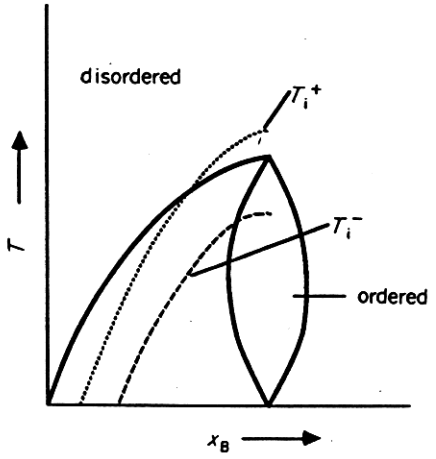

Figure 9
Simplified phase diagram for a first-order O–D transition, showing instability lines

7. Deformation of Ordered Phases

Slip in an ordered phase is usually more difficult than slip in its disordered parent structure. This is so because a moving dislocation, whose Burgers vector is determined by the disordered repeat distance, would destroy the atomic order in the ordered structure. Thus, dislocations in ordered structures need to have larger Burgers vectors, $|b|$, to represent the decrease in translational symmetry which occurs on ordering. Larger $|b|$ mean the self energy of dislocations in ordered structures is larger, and hence the dislocations are more difficult to form, as well as more difficult to move, once they are formed.

Twinning is another mechanism of deformation in crystalline alloys. Twinning of the bcc and fcc structures is well documented. Thus, the most prevalent twinning mode for bcc is denoted as 2.2^T and for fcc is written as 2.2. If the mode 2.2^T is applied to the B2 structure, a new structure is formed (*Cmmm*). This structure has near-neighbor B–B bonds, and is thus presumed to be of higher energy. The same is true for the application of 2.2 mode to the $L1_2$ structure. In fact, for each of the cubic structures B2, DO_3, B32 and $L1_2$, the application of the twinning mode of the corresponding disordered parent structure produces a new structure of orthorhombic symmetry. There is therefore a driving force for it to "untwin" and return to its original shape. Most shape-memory alloys (see *Shape-Memory-Effect Alloys: Basic Principles*) are composed of phases with structures that can not be twinned through their disordered twinning mode.

See also: Alloy Crystal Structures and Their Stability; Crystal Structure Determination; Interstitial Ordering in Alloys; Local Order in Crystalline Alloys; Metallic Solid Solutions: Phase Separation (Suppl. 1)

Bibliography

Aaronson H I, Laughlin D E, Sekerka R F, Wayman C E (eds.) 1982 *Solid–Solid Phase Transformations*. The Metallurgical Society of AIME, Warrendale, Pennsylvania

Allen S M, Cahn J W 1982 Phase diagram features associated with multicritical points in alloy systems. *Bull. Alloy Phase Diagrams* 3: 287–95

Binder K (ed.) 1986 *Monte Carlo Methods in Statistical Physics*, Series in Solid State Science, Vol. 7. Springer, Berlin

Christian J W 1975 *The Theory of Transformations in Metals and Alloys*, 2nd edn. Pergamon, Oxford

De Fontaine D 1979 Configurational thermodynamics of solid solutions. *Solid State Phys.* 34: 73–274

Gahn U 1986 Ordering in face-centered cubic binary crystals confined to nearest-neighbor interactions—Monte Carlo calculations. *J. Phys. Chem. Solids* 47: 1153–69

Khachaturyan A G 1978 Ordering in substitutional and interstitial solid solutions. *Prog. Mater. Sci.* 22: 1–150

Khachaturyan A G 1983 *The Theory of Structural Transformations in Solids*. Wiley, New York

Kikuchi R 1951 A theory of cooperative phenomena. *Phys. Rev.* 81: 988–1003

Krivoglaz M A, Smirnov A A 1969 *The Theory of Order–Disorder in Alloys*. Macdonald, London

Landau L D, Lifshitz E M 1978 *Statistical Physics*. Pergamon, Oxford

Martins J L, Zunger A 1986 Ordering and decomposition in semiconductor alloys. *J. Mater. Res.* 1: 523–26

Richards M J, Cahn J W 1971 Pairwise interactions and the ground state of ordered binary alloys. *Acta Metall.* 19: 1263–77

Sanchez J M, Ducastelle F, Gratias D 1984 Generalised cluster description of multicomponent systems. *Physica A* 128: 334–50

Warlimont H (ed.) 1974 *Order–Disorder Transformations in Alloys*. Springer, Berlin

D. E. Laughlin
[Carnegie Mellon University, Pittsburgh, Pennsylvania, USA]